Proceedings of the International Conference on Applied Mechanical Engineering Research (IC-AMER2019)
NIT Warangal, India – May 02-05, 2019
Paper No. XXX (The number assigned when the paper is accepted)

Comparative study of various defects in monolayer graphene using molecular dynamics simulation

Kritesh Kumar Gupta[a,*], Aditya Roy[b], Sudip Dey
[a,b,c] *Department of Mechanical Engineering, National Institute of Technology Silchar, 788010, Assam, India*

*Corresponding author Email: kriteshamie@gmail.com

The present study uses the molecular dynamics approach to study the various defects available in graphene sheet and, also records its effect on the strength and stiffness of graphene. The graphene sheet is uniaxially deformed in its armchair and zigzag direction. In order to examine the fracture behaviour of defective graphene, molecular dynamics (MD) simulations based on AIREBO interatomic potential field and Nose-Hoover thermostat and barostat techniques are implemented. The present study shows that with the introduction of the defects the fracture/yield strength of graphene reduces up to some extent in both of its direction. However, the presence of crack reduces the strength of graphene significantly more. Further, the study also concludes that the graphene withholds much higher stress when loaded in its zigzag direction in comparison with loading it in armchair direction.

***Keywords*:** molecular dynamics simulations, monolayer graphene, defects

Introduction

The extraordinary characteristics of graphene have been used to develop nanoresonators[1], biosensors[2], nanocomposites[3] and many more nanoelectromechanical systems (NEMS). Very first time Professor Sir Andre Geim and Professor Sir Kostya Novoselov extracted the single layer graphene sheet (SLGS) from graphite in 2004. Since then graphene has been explored by a lot of researchers in order to determine its exact mechanical properties and strength. After the invention of graphene, it Lee et al. in 2008 experimentally found that the graphene is one of the lightest (0.77 mgm^{-2}) and still stiffest material known. Its fracture strength and Young's modulus were recorded as 130 GPa and 1 TPa, respectively[4]. Experimentally one of the common methods to extract graphene from graphite is CVD (Chemical Vapor Decomposition), which is performed at elevated temperatures. It is obvious that during extraction some defects may be introduced to the graphene structure by vacancy, chemical reactions with foreign elements or by a change in the bond structure at elevated temperatures. This leads to getting incorrect desired results from the experimentation. The irregularities in the graphene structure remarkably reduce the strength of graphene, which in return may affect the performance of the NEMS. In past, researchers have made a lot of efforts to gather the exact characteristics of graphene. Such as Tsai et al. [5] determined the elastic properties of the SLGS and graphite flakes through molecular dynamics simulation. They concluded that the single graphene layer has a higher value of stiffness and shear modulus when compared with that of graphite flakes. Scarpa et al.[6] calculated the elastic moduli of SLGS using analytical models of truss and the theory of cellular material mechanics while Thomas et al.[7] performed the large atomistic simulation using MD (molecular dynamics) simulation and tersoff interatomic potential and determined the mechanical, thermal and structural properties of the single-layered graphene. In contrast, Ansari et al. [8] performed the atomistic simulation using MD and Tersoff-Brenner potential energy function to determine the mechanical properties of perfect and defective single-layered graphene while Dewapriya and Rajapakse [9] investigated failure criteria of SLGS depending on the rate of strain and temperature. They proposed a fracture mechanics model based on the continuum to characterize the strength of defected graphene. Wang et al. [10] examined the

failure strength of Stone-Wales defected graphene using molecular dynamic simulation, the study was carried out at various temperature and it was concluded that the strength of SLGS is affected by the presence of defects, loading directions and temperature. Anastasi et al. [11] presented the MD simulation of single-layer graphene under tensile loading in a single direction. In order to carry out the simulation, several potential functions such as the bending angle, Morse, Lennard-Jones and torsion potential functions have been used from the mdFOAM library of OPENFOAM software. It was concluded from the study that graphene is anisotropic, and its fracture strength depends on the sheet size. Wang et al. [12] investigated the mechanical responses of the graphene membrane with 5-8-5 defect using MD simulation. It was concluded from the study that by introducing a 5-8-5 defect in graphene sheet the fracture strength and strain become smaller. Fenley et al. [13] developed the software to calculate the atomistic mechanical stress to be used in the MD simulations of bimolecular and nanomaterials using AMBER interatomic potential function. Clavier et al. [14] computed the elastic stiffness tensor at 1 bar and 60K of FCC argon through MD simulation. They also compared the result obtained by using NPT and NVT ensembles of MD. To use the monolayer graphene as the reinforcements in composite Papageorgio et al. [15] reviewed its mechanical properties. They described the strategies to prepare the bulk graphene-based nanocomposites. It was concluded from the study that graphene as the reinforcement in composites may improve the strength of the composite up to the next level. Singh et al. [17] predicted the elastic properties of the graphene sheet at infinitesimal and finite strains by combining MM3 potential with the Cauchy-Born rule. They further compared the results with the outcome of a study carried out using various popular potential fields such as Tersoff-Brenner and AIREBO. Shao et al. [18] did the analysis of the varying ultimate strength, thermal expansion coefficients, lattice geometries, and elastic constants with respect to the temperature of graphyne and graphene by combining first-principles calculation with a quasi-harmonic approximation. The modelling of nanomaterials helps in analyzing the actual characteristics of the material in a better manner. It is because of the fact that user can regulate critical parameters such as temperature, pressure etc. using the tools available. In physical experimentation, regulating these critical parameters becomes an expensive and tedious task to perform. Therefore using MD simulation as the analysis tool gives the edge over, understanding the complex nanomaterials in a better way. The present study, analyze the strength and stiffness of the perfect SLGS along with the graphene with various defects such as single vacancy, Stone-Wales defect, nanopore, and crack, using MD simulation. The modulus of elasticity, fracture stress, and failure strain are determined for both armchair and zigzag directions of graphene. The strength and mechanical properties of defective graphene are further compared with those of perfect graphene.

1. Molecular Dynamics Simulation

1.1. Numerical Methodology

The nanomechanical modelling is one of the best methods to analyze the properties of nanomaterials; it can be differentiated into three main categories- The first principle approaches such as density functional theory (DFT), semi-empirical methods such as molecular dynamics simulation and the third one is the modified continuum model. The molecular dynamics is computationally affordable in comparison with the first-principles approaches. Apart from that MD is extremely fast and can handle much larger systems when compared with the first-principle methods. Although MD relies on several assumptions associated with the interatomic potential function. The interatomic potential functions are created by the calibration of previous experimental results using the curve fitting methods. These interatomic potential functions describe the interactions between the constituent atoms. The MD simulation considers the material as the collection of individual atoms which interact by exerting forces on each other and follow Newton's law of motion. The simulation procedure in MD initiates by determining the force acting on an individual atom by the neighbouring atoms. Force acting on atom *i*-

$$f_i = -\frac{\partial E_i}{\partial r_i} \tag{1}$$

where E_i represents the potential energy of atoms. The potential energy between the atoms is approximated by interatomic potential field. After the determination of forces, the accelerations are determined using Newton's equation of motion-

$$f_i = m_i \frac{d^2 r_i}{dt^2} = m_i a_i \tag{2}$$

Further, the atoms are allowed to accelerate for a certain duration, known as timestep. At the end of each timestep, the new positions and velocities are determined using numerical integration algorithms such as velocity Verlet. The use of statistical ensemble such as NPT, NVT, NVE etc. allows controlling the temperature and pressure of the system [25].

1.2. Modelling and Simulation

We used the open source software VMD (Visual Molecular Dynamics) [22] for modelling the square shape perfect graphene sheet of 5-nanometer edge length with 1008 carbon atoms. Figure 1 shows the topology of the perfect graphene with its armchair and zigzag directions. The output file received from VMD is fed to Avogadro [23] (an open source atom manipulator) in order to introduce the vacancy defect, Stone-Wales defect, nanopore and crack in the perfect graphene sheet. The *data files* containing the coordinates of atoms were generated by using the *topotool* plugin of VMD.

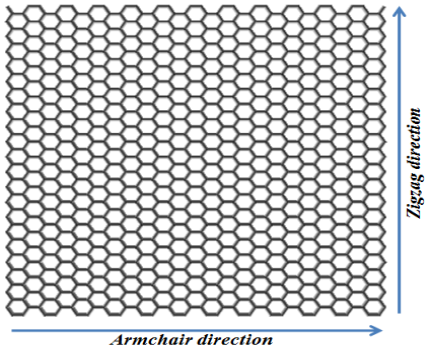

Fig. 1. The topology of the perfect graphene sheet

Figure. 2 depicts the various defects considered in the fracture analysis. The Stone-Wales defect shown in figure 2*(b)* is formed by a bond rotation of 90 degrees between two adjacent carbon atoms, which results in the formation of pentagon-septagon pairs. The nanopore shown in figure 2*(c)* has the dimension 5.63 angstroms in the armchair direction and 7.36 angstrom in the zigzag direction. And the crack shown in figure 2*(d)* has the length 12.28 angstrom and width 4.25 angstrom.

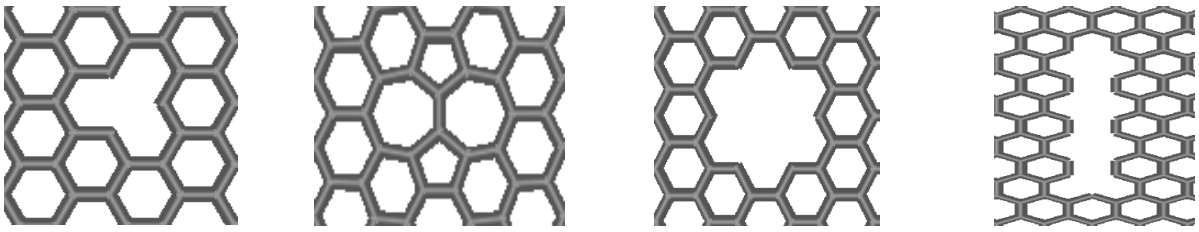

(a) *(b)* *(c)* *(d)*

Fig. 2. Defected graphene with *(a)* single vacancy, *(b)* Stone-Wales defect, *(c)* nanopore, *(d)* crack.

Both the sheets (perfect and defected) were uniaxially deformed in an armchair and zigzag direction using LAMMPS which is an acronym of Large-scale Atomic/Molecular Massively

Parallel Simulator. It is an open source code by Sandia National Laboratories USA. To avoid free edges, all three directions were applied with periodic boundary conditions. The sheets were firstly equilibrated to minimize the energy of the system, over 60 picoseconds before applying strain, using timestep of 1 femtosecond. In the relaxation period, the pressure component of the x and y directions was maintained zero using NPT ensemble. The NPT uses Nose-Hoover technique to maintain the desired temperature and pressure of the system. Furthermore, to uniaxially deform the sheets a strain was imposed by elongation of the simulation box in both (armchair and zigzag) dimension and the applied strain rate was $10^9 s^{-1}$. The stress components in y and z directions were kept at zero during simulating the tensile deformation of graphene by keeping in check the pressure component in the said directions using NPT ensemble.

1.3. Interatomic Potential Function

In molecular dynamics simulation, the potential field or function is an element which signifies the energy interactions between the atoms. The adaptive intermolecular reactive empirical bond order (AIREBO) potential is employed in the present study for the analysis of perfect, defective and doped graphene. The AIREBO potential has an advantage of usage in molecular dynamics simulation due to the fact it covers the maximum interaction criteria between the carbon atoms. The AIREBO potential is made by combining three different potential fields. First, the original REBO potential, second, the Lenard-Jones (LJ) and third, the torsion potential. The original REBO term imparts the inter-atomic attractive and repulsive energy, the Lennard-Jones to account for the intermolecular interaction that includes dispersion and short-range repulsion and torsion component to signify the torsional interactions between single bonds. The general form to represent the AIREBO potential is- [21]

$$E = \frac{1}{2}\sum_{i=1}\sum_{i\neq j}[E_{ij}^{REBO} + E_{ij}^{LJ} + \sum_{k\neq i}\sum_{l\neq i,j,k} E_{ijkl}^{TORSION}] \tag{3}$$

where E refers to the total potential energy with atoms *i*, *j*, *k*, and *l*. The REBO term, which accounts for interatomic attraction and repulsion is represented as:

$$E_{ij}^{REBO} = V_{ij}^{R}(r_{ij}) + b_{ij}V_{ij}^{A}(r_{ij}) \tag{4}$$

where V^A and V^R refer the attractive and repulsive parts of the potential respectively; r_{ij} signifies the distance between *i* and *j* atom up to the cutoff distance and b_{ij} refers the bond order which allows for a change in the strength of the bond as per the restrictions due to external factors. The LJ term of the potential can be described as:

$$E_{ij}^{LJ} = f(r_{ij})V_{ij}^{LJ} \tag{5}$$

$$V_{ij}^{LJ} = 4\varepsilon_{ij}\left[\left(\frac{\sigma_{ij}}{r_{ij}}\right)^{12} - \left(\frac{\sigma_{ij}}{r_{ij}}\right)^{6}\right] \tag{6}$$

where $f(r_{ij})$ represents the set of cutoff functions and σ_{ij} *and* ε_{ij} are the distance of zero interatomic potential and the potential barrier respectively. Finally, the torsion term can be represented as:

$$E_{ijkl}^{TORSION} = f(r_{ij}, r_{jk}, r_{kl})V^{TORSION}(w_{ijkl}) \tag{7}$$

$$V^{TORSION}(w_{ijkl}) = \varepsilon\left[\frac{256}{405}\cos^{10}\left(\frac{w}{2}\right) - \frac{1}{10}\right] \tag{8}$$

where r_{ij}, $r_{jk,}$ and r_{kl} are the bond lengths, w_{ijkl} is the dihedral angle and ε is the barrier height of the potential.

1.4. Calculation of stresses

In the molecular dynamic simulation, stress may be interpreted as Cauchy stress or virial stress. When it comes to the computational efficiency the Cauchy stress is proved to be more considerable than virial stress. Although, some amount of initial stress (when strain is zero) is induced by the Cauchy stress at higher temperatures. In this study, the computation of virial stress is carried out through atomistic simulation. Virial stress can be defined as [9]:

$$\sigma_{ij} = \frac{1}{V}\sum_{\alpha}\left[\frac{1}{2}\sum_{\beta=1}^{N}\left(R_i^{\beta} - R_i^{\alpha}\right)F_j^{\alpha\beta} - m^{\alpha}v_i^{\alpha}v_j^{\alpha}\right] \quad (9)$$

where α and β refer to the number assigned to an atom and the number assigned to the neighboring atom, respectively; while i and j signify the directional indices, m^{α} and v_i^{α} are the mass and velocity of the atom α, respectively. R_i^{β} is the location of atom β in i direction; $F_j^{\alpha\beta}$ is the force due to an atom β on atom α along the j direction; V refers to the total volume of the material system. The virial stress represents a product of stress and volume i.e., the stress value computed by LAMMPS would be in the units of pressure*volume, in order to extract the stress from the computed value it is essential to divide the value calculated by the LAMMPS with the total volume. Furthermore, in order to calculate the virial stress, the instantaneous volume is used i.e. when the imposed strain is 'ε', the value of volume at the given instant would be $V_0(1+\varepsilon)$, where V_0 represents the initial volume of the system.

2. Results and Discussion

The Young's modulus, elastic constants, Poisson's ratio, and ultimate strength are determined and show a good agreement with the literature values. The aforesaid values are determined for the perfect graphene, which is expressed as follows-

Table. 1. Validation of the present study

Properties	**Present study**	**Literature values**
C11 (in GPa)	1033.7	1094 (Thomas et al. 2014)
C12 (in GPa)	142.6	136 (Thomas et al. 2014)
Young's modulus (in TPa)	1.014	1.020 (Lee et al. 2008)
Poisson's ratio	0.1379	0.1248 (Thomas et al. 2014)
Fracture strength (in GPa)	165.7	130 (Lee et al. 2008)

The stress-strain behaviour of perfect and defective graphene is recorded in the armchair and zigzag directions. The stress-strain plots are illustrated in figure 3-

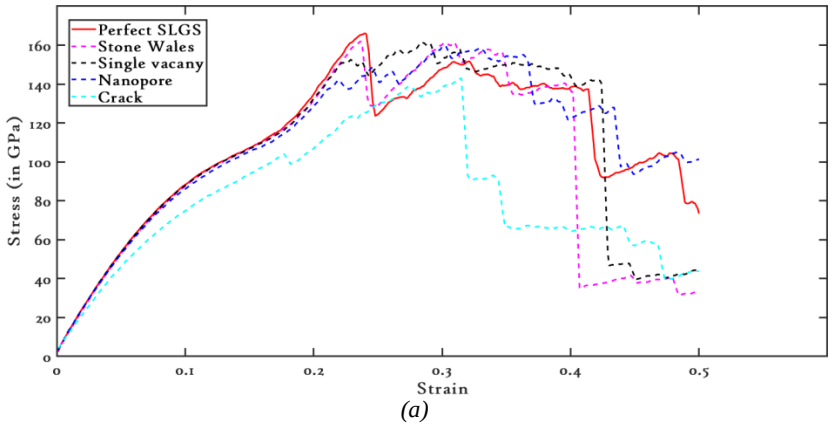

(a)

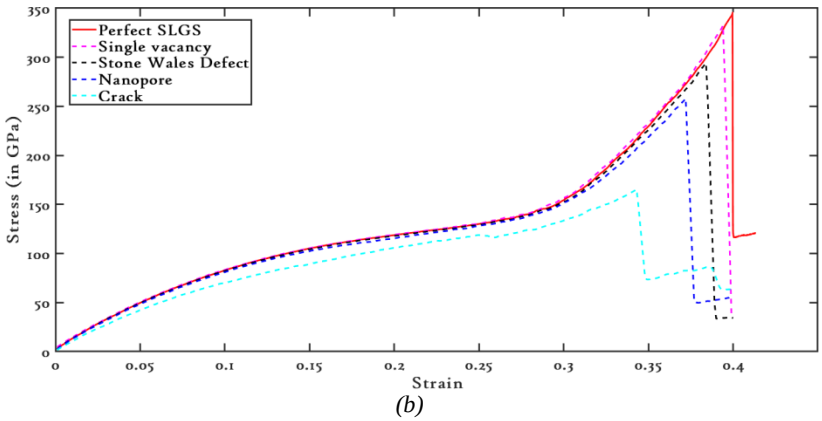

(b)

Fig. 3. Stress-Strain behaviour of perfect and defective graphene in *(a)* armchair direction, *(b)* zigzag direction

It is evident from the stress-strain behaviour of the perfect and defective graphene in both the directions; the zigzag direction has a higher fracture strength. It is also clear that the defective graphene shows considerable yielding prior failure when loaded in the armchair direction. However, the defects do not affect much Young's modulus of graphene, apart from the crack which shows a drastic reduction in Young's modulus of the graphene. The stress-strain behaviour shows that failure strain is high in case of loading in a zigzag direction. This shows that the zigzag direction graphene shows more resistance to failure; as. Table 2 and Table 3 show the values of elastic constants, modulus of elasticity, Poisson's ratio and fracture strength of the perfect and defective graphene sheet in an armchair and zigzag directions respectively. From the comparison of mechanical properties in an armchair and the zigzag direction, it is clear that the graphene is stiffer in armchair direction and stronger in a zigzag direction.

Table. 2. Comparison of mechanical properties in armchair direction

	C_{11} (in GPa)	**C_{12} (in GPa)**	**Young's modulus (in TPa)**	**Poisson's ratio**	**Fracture strength (in GPa)**
Perfect SLGS	1074.08	169.04	1.047	0.1573	165.7
Stone-Wales defect	1058.34	181.90	1.027	0.1718	161.9
Vacancy defect	1070.78	123.90	1.056	0.1157	151.1
Nanopore	1055.86	164.92	1.030	0.1562	141.4
Crack	935.32	180.16	0.9	0.192	143.1

Table. 3. Comparison of mechanical properties in zigzag direction

	C_{11} (in GPa)	**C_{12} (in GPa)**	**Young's modulus (in TPa)**	**Poisson's ratio**	**Fracture strength (in GPa)**
Perfect SLGS	1025	273.29	0.952	0.266	346.2
Stone-Wales defect	1009.12	253.46	0.945	0.251	332.2
Vacancy defect	992.99	257.94	0.925	0.259	294.2

Nanopore	970.43	235.86	0.913	0.243	257.9
Crack	848.67	233.83	0.784	0.275	165.2

3. Conclusion

The present study uses the MD simulations to uniaxially deform the perfect and defective (Stone-Wales defect, vacancy defect, nanopore, and crack) SLGS in both of its loading directions. The AIREBO potential is used to incorporate the interatomic interactions between the constituent atoms. The Nose-Hoover barostat is used to control the atomistic pressure of the system by using the NPT ensemble. The mechanical properties of the perfect and defective graphene sheet are observed in both the directions and it is concluded that defects have the profound impact on the strength of graphene in both the directions, whereas it does not affect the stiffness much; apart from the case of crack present in graphene. It is also seen that the graphene has more resistance to failure in its zigzag direction than armchair direction. However, the graphene has a high value of stiffness in its armchair direction. It is also evident that by introducing defects in graphene and loading it in armchair direction; graphene shows the considerable yielding before failure which remains absent in zigzag direction.

References

1. M. D. Dai, C. W. Kim, K. Eom, Nonlinear vibration behaviour of graphene resonators and their applications in sensitive mass detection, Nanoscale Research Letters, 7(1), (2012).
2. T. Kuila, S. Bose, P. Khanra, A. K. Mishra, N.H. Kim, J.H. Lee, Recent advances in graphene-based biosensors. Biosensors and Bioelectronics, 26, 4637– 4648 (2011).
3. G. Wang, B. Wang, X. Wang, J. Park, S. Dou, H. Ahn, and K. Kim, Sn/graphene nanocomposite with 3D architecture for enhanced reversible lithium storage in lithium ion batteries, Journal of Materials Chemistry, 19, 8378-8384 (2009).
4. C. Lee, X. Wei, J.W. Kysar, and J. Hone, Measurement of the elastic properties and intrinsic strength of monolayer graphene. Science, 321, 385–388 (2008).
5. J.L. Tsai, J.F. Tu, Characterizing mechanical properties of graphite using molecular dynamics simulation. Materials and Design, 31, 194-199 (2010).
6. F. Scarpa, S. Adhikari, A.S. Phani, Effective elastic mechanical properties of single-layer graphene sheets, Nanotechnology, 20, (2009).
7. S. Thomas, Ajith K.M., Molecular dynamics simulation of the thermomechanical properties of the monolayer graphene sheet, Proc. Materials Sci., 5, 489-498 (2014).
8. R. Ansari, S. Ajori, B. Motevalli, Mechanical properties of defective single-layered graphene sheets via molecular dynamics simulation, Superlattices and Microstructures, 51, 274-289 (2012).
9. M.A.N. Dewapriya, R.K.N.D. Rajapakse, Molecular dynamics simulations and continuum modeling of temperature and strain rate dependent fracture strength of graphene with vacancy defects, Journal of Applied Mechanics, 81, (2014).
10. M.C. Wang, C. Yan, L. Ma, N. Hu, M.W. Chen, Effect of defects on the fracture strength of graphene sheets, Computational Materials Science, 54, 236-239 (2012).
11. A.A. Anastasi, K. Ritos, G. Cassar, M.K. Borg, Mechanical properties of pristine and nanoporous graphene, Molecular Simulation, (2016).
12. S. Wang, B. Yang, J. Yuan, Y. Si, H. Chen, Large-Scale Molecular Simulations on the Mechanical Response and Failure behavior of a defective Graphene: Cases of 5-8-5 Defects, Scientific Reports, (2015).
13. A.T. Fenley, H.S. Muddana, M.K. Gilson, Calculation and visualization of atomistic mechanical stresses in nanomaterials and biomolecules, PLoS ONE, 9(12), (2014).

14. G. Clavier, N. Desbiens, E. Bourasseau, V. Lachet, N. Brussel-Dupend, B. Rousseau, Computation of elastic constants of solids using molecular simulation: comparison of constant volume and constant pressure ensemble methods, Molecular Simulation, 43, 1413-1422 (2017).
15. D.G. Papageorgio, I.A. Kinloch, R.J. Young, Mechanical properties of graphene and graphene-based nanocomposites, Progress in Material Science, 90, 75-127 (2017).
16. A. Carpio, L.L. Bonilla, F. di Juan, M.A.H. Vozmediano, Dislocations in graphene, New Journal of Physics, 10(5) (2008).
17. S. Singh, B.P. Patel, Nonlinear elastic properties of graphene sheet using MM3 potential under finite deformation, Composites Part B, 136, 81-91 (2018).
18. T. Shao, B. Wen, R. Melnik, S. Yao, Y. Kawazoe, Temperature-dependent elastic constants and ultimate strength of graphene and graphyne, J. Chem. Physics, 137 (2012).
19. M.M. Zaeri, S. Ziaei-Rad, Molecular dynamics investigation of the elastic constants and moduli of single-walled carbon nanotubes, J. Nanoanalysis, 4(1), 65-75 (2017).
20. A. P. Thompson, S.J. Plimpton, W. Mattson, General formulation of pressure and stress tensor for arbitrary many-body interaction potentials under periodic boundary conditions, Journal of Chemical Physics, 131 (2009).
21. S.J. Stuart, A.B. Tutein, J.A. Harrison, A reactive potential for hydrocarbons with intermolecular interactions, Journal of Chemical Physics, 112(14) (2000).
22. W. Humphrey, A. Dalke, K. Schulten, VMD- Visual Molecular Dynamics, J. Molec. Graphics, vol. 14, pp. 33-38 (1996).
23. M.D. Hanwell, D.E. Curtis, D.C. Lonie, T. Vandermeersch, E. Zurek, G.R. Hutchison, Avogadro: An advanced semantic chemical editor, visualization, and analysis platform, Journal of Cheminformatics, 4(17), (2012).
24. W. Cai, Introduction to Molecular Simulations – Stanford Univ., USA (2007, Winter).
25. J.G. Lee, Computational Materials Science An Introduction, 2nd Edition, CRC Press, Florida (2017)